where Π is the self-energy. Near the mass shell we have

$$\Pi = m^2 - m_0^2 + (p^2 - m^2)(d\Pi/dp^2)$$

whereupon Eq. (7) becomes

$$\lim_{p^2 \to m^2} \bar{\Gamma}_{\lambda\mu} = [-(p^2 - m^2) g_{\lambda\mu}{}^0 + 2p_\lambda p_\mu][1 - d\Pi/dp^2]. \quad (8)$$

Thus in the long-wavelength limit the coupling is the same as with a noninteracting field of mass m, multiplied by the vertex renormalization factor $[1-d\Pi/dp^2] = Z_1^{-1}$. In usual fashion this factor is taken out by the renormalization factors of $S(p)$ [cf. Eq. (5)], so that the Ward identity simply reduces to $Z^{-1}Z_2 = 1$ when one uses the renormalized mass. This result implies the universality of the gravitational coupling to the energy momentum tensor calculated with the true inertial mass (for particles on the mass shell) whatever the origin of the mass and independent of the Lagrangian of the gravitational field. This is the expression of the principle of equivalence. Off the mass shell, Eq. (6) is the appropriate generalization of the principle of equivalence.

We close with two remarks: (1) On the basis of a previous paper,[5] it is possible that theories which break Lorentz invariance[6] lead to a graviton mass. (2) Because of the Ward identity, it is probable that gravitation is a renormalizable theory. We hope to return to these problems as well as to the question of the meaning of a flat space in a filled universe in subsequent work.

We should like to express our gratitude to Professor D. Speiser of the University of Louvain who alerted us to the link between our Ward identity and the principle of equivalence. One of us (R.B.) wishes to acknowledge a stimulating discussion with Professor H. Bondi of King's College on the subject matter of this paper.

[5] F. Englert and R. Brout, Phys. Rev. Letters **13**, 321 (1964).
[6] For example J. Bjorken, Ann. Phys. (N. Y.) **24**, 174 (1963); I. Bialynicki-Birula, Phys. Rev. **130**, 465 (1963).

PHYSICAL REVIEW VOLUME 141, NUMBER 4 JANUARY 1966

Hydrodynamic Calculations of General-Relativistic Collapse*

MICHAEL M. MAY AND RICHARD H. WHITE
Lawrence Radiation Laboratory, University of California, Livermore, California
(Received 19 August 1965)

The general-relativistic equations governing the motion of a large mass under the influence of its own gravitational field and its own pressure have been approximated by finite-difference equations. A spherically symmetric, co-moving frame of reference was used. The pressure was assumed to be zero at the outer boundary. Rest mass was assumed to be conserved and heat transfer by neutrinos, radiation, etc., was not taken into account. Numerical solutions were obtained on a computer for several simplified equations of state, chosen to bracket the behavior of stellar material in late stages of collapse, and several masses. The maximum stable masses obtained were of the same order of magnitude, but somewhat larger than the maximum stable masses calculated statically. The behavior of light signals, of the metric coefficients, and of the hydrodynamic quantities as functions of time is described for collapse past the Schwarzschild radius. Such collapse leads to regions where the surface area of concentric spheres decreases as the rest mass contained by the spheres increases.

I. INTRODUCTION

THE gravitational collapse of spherically symmetric masses under conditions where the general theory of relativity is expected to apply has been calculated by solving the field equations in finite-difference approximation on digital computers. This paper presents results of this calculation for materials with simple equations of state and for simple initial and boundary conditions. The purpose is to provide a description of the collapse in the presence of nonzero pressures, and to verify current estimates of maximum stable mass. The calculation can be extended to take into account pair production, heat transfer, and other mechanisms of interest for the description of astrophysical processes.

* Work performed under the auspices of the U. S. Atomic Energy Commission.

II. EQUATIONS

We consider an ideal fluid and neglect all heat transfer except that due to the motion of the fluid itself. The specific entropy of the fluid at a given mass point is then constant except when the mass point goes through a shock. We neglect pair production and annihilation, and the interaction of the fluid with external fields, so that rest mass is conserved. Assuming spherical symmetry leads to the metric[1]

$$ds^2 = a^2(\mu,t)c^2dt^2 - b^2(\mu,t)d\mu^2 - R^2(\mu,t)d\Omega^2, \quad (1)$$

[1] L. D. Landau and E. M. Lifshitz, *The Classical Theory of Fields* (Addison-Wesley Publishing Company, Reading, Massachusetts, 1962), 2nd ed., pp. 331–332.

where $d\Omega^2 = d\theta^2 + \sin^2\theta d\phi^2$, μ is a radial coordinate, and $2\pi R(\mu,t)$ is the circumference of a circle going through points of a given μ at time t. Choosing a coordinate system which moves with the fluid leads to the energy momentum tensor:

$$T_1{}^1 = T_2{}^2 = T_3{}^3 = P, \quad T_0{}^0 = -\rho(c^2+\epsilon), \tag{2}$$

where P is the pressure, ϵ the internal energy per gram, and ρ the rest mass density of the separated particles making up the fluid, i.e., the rest mass excluding ϵ/c^2. If μ is defined as the rest mass between the point labeled and the center, the assumption of rest-mass conservation becomes

$$4\pi\rho R^2 b = 1, \tag{3}$$

and the Einstein field equations become:

$$(T_0{}^0) \quad 4\pi G\rho\left(1+\frac{\epsilon}{c^2}\right)R^2R' = \frac{c^2}{2}\left(R+\frac{R\dot{R}^2}{a^2c^2}-\frac{RR'^2}{b^2}\right)' \equiv m'G, \tag{4}$$

$$(T_1{}^1) \quad \frac{4\pi G}{c^2}PR^2\dot{R} = -\frac{c^2}{2}\left(R+\frac{R\dot{R}^2}{a^2c^2}-\frac{RR'^2}{b^2}\right)^{\cdot} = -\dot{m}G, \tag{5}$$

$$(T_2{}^2, T_3{}^3) \quad 4\pi G\rho wR^3 = c^2\left(R+\frac{R\dot{R}^2}{a^2c^2}-\frac{RR'^2}{b^2}\right) + \frac{R^3c}{ab}\left[\left(\frac{a'c}{b}\right)' - \left(\frac{\dot{b}}{ac}\right)^{\cdot}\right], \tag{6}$$

$$(T_0{}^1, T_1{}^0) \quad 0 = \frac{a'\dot{R}}{a} + \frac{\dot{b}R'}{b} - \dot{R}', \tag{7}$$

where $\cdot$ means $\partial/\partial t$, $'$ means $\partial/\partial\mu$, and w, the specific enthalpy, is

$$w = (1+\epsilon/c^2+P/\rho c^2). \tag{8}$$

Shown in parentheses to the left of Eqs. (4) through (7) are the energy momentum tensor components involved. We have introduced into (4) and (5) the total mass up to point μ

$$m(\mu,t) = 4\pi\int_0^\mu \rho(1+\epsilon/c^2)R^2R'd\mu. \tag{9}$$

Defining also

$$u = \dot{R}/a, \tag{10}$$

$$\Gamma = 4\pi\rho R^2R', \tag{11}$$

Eq. (4) can be integrated from 0 to μ, giving

$$\Gamma^2 = 1+(u/c)^2-(2mG/Rc^2). \tag{12}$$

u is the 1-component of the 4-velocity in a Schwarzchild coordinate system[2] defined by the metric

$$ds^2 = e^\nu c^2 d\tau^2 - e^\lambda dR^2 - R^2 d\Omega^2. \tag{13}$$

If G were zero, Γ would become the $\gamma = (1-v^2/c^2)^{-1/2}$ of special relativity corresponding to the Lorentz transformation connecting, at a given time, the coordinate systems defined by (1) and (13).

The divergence equations $T_i{}^k{}_{;\,k} = 0$ are

$$(T_0{}^k{}_{;\,k}) \quad [\rho(1+\epsilon/c^2)]^{\cdot} + [(\dot{b}/b)+(2\dot{R}/R)]\rho w = 0, \tag{14}$$

$$(T_1{}^k{}_{;\,k}) \quad P' + (a'/a)\rho wc^2 = 0. \tag{15}$$

Of the six equations: (4) through (7), (14), and (15), only four are independent. Using (3) in (14) gives

$$\dot{\epsilon} + P(1/\rho)^{\cdot} = 0. \tag{16}$$

Using (12), (7) for $\dot{R}'$, and (15) for a', (5) becomes the equation of motion:

$$\dot{u} = -a(4\pi P'R^2(\Gamma/w) + (mG/R^2) + (4\pi PGR/c^2)). \tag{17}$$

Using (3), (7) becomes the equation of mass conservation

$$(\rho R^2)^{\cdot}/\rho R^2 = -a(u'/R'). \tag{18}$$

These equations have been obtained independently and discussed by Misner and Sharp.[3] Equations (15) through (18), together with the definitions of u, Γ, m, and w, and the equation of state, determine the solution of the problem of spherically symmetric fluid motion, with rest mass conservation and no heat transfer. Taking derivatives with respect to local clock time, $(1/a)\partial/\partial t$, to be equivalent to time derivatives in the nonrelativistic limit, Eqs. (16) through (18) are seen to differ from the nonrelativistic equations of energy conservation, motion, and continuity, respectively (in Lagrangian coordinates), only through the introduction, into the equation of motion (17), of the factor Γ/w multiplying the pressure gradient and of the added gravitational term $4\pi PGR/c^2$.

These equations were solved on digital computers (mainly the CDC-3600), using a finite-difference method similar to the one generally used for solving hydrodynamic problems in a Lagrange coordinate system.[4] Mathematical details of the method will be made available elsewhere. Shocks were treated by means of an artificial viscosity, similar to that of Richtmyer and von Neumann,[5] that is, by means of a scalar stress which is zero where no pressure or density discontinuity tends to form, and spreads the discontinuity over three or four zones where it does tend to form. For the description of complete collapse, it makes no difference whether an artificial viscosity is introduced or not; such an artificial viscosity is never operative.

---

[2] Reference 1 pp. 327 ff.
[3] C. W. Misner and D. H. Sharp, Phys. Rev. **136**, B571 (1964).
[4] R. D. Richtmyer, *Difference Methods for Initial Value Problems* (Interscience Publishers, New York, 1957) Chap. X.
[5] J. von Neumann and R. D. Richtmyer, J. Appl. Phys. **21**, 232 (1950).

Initial conditions for these equations were varied. The boundary conditions used were

$$P=0,\quad a=1 \text{ at } \mu=\mu_{\max},$$
$$u=0,\quad R=0 \text{ at } \mu=0. \tag{19}$$

The condition $a=1$ at $\mu=\mu_{\max}$ makes coordinate time equal to the clock time of an observer moving with the outer boundary. This boundary, in the problems run so far, did not come into a region where general relativistic effects were important, even when the inner part of the material collapsed completely.

The conditions at $\mu=0$ lead to $\Gamma(\mu=0)=1$, if ρ and ϵ are not to be infinite there.

III. RESULTS

A. Collapse versus "Bounce." Mass Loss

Consider material at rest and in local thermodynamic equilibrium. Let the total rest mass of the separated particles making up the material be $\mu_{\max}$ and its total energy be Mc^2. If the assembly is not in hydrostatic equilibrium and $M < \mu_{\max}$, gravitational collapse begins. If there is no external interaction, and no radiation or other mass loss, both M and $\mu_{\max}$ remain constant, as does therefore their difference, the binding energy

$$B=(\mu_{\max}-M)c^2=\int_0^{\mu_{\max}}[c^2-\Gamma(c^2+\epsilon)]d\mu. \tag{20}$$

Even if M is below the maximum stable mass for the material in question (e.g., in the case of cold neutrons, below 0.72 $M_\odot$, the Oppenheimer-Volkoff limit[6]), the assembly is not expected to settle into the equilibrium configuration appropriate to its mass and initial entropy. It will have too little binding energy. Except for radiation and mass loss, it seems likely to oscillate about an equilibrium point, until viscous damping transforms enough of the excess kinetic energy into heat for the material to come into hydrostatic equilibrium at a higher entropy than the initial one.

If M is above the maximum stable equilibrium mass, there may still be a range of masses for which collapse will not occur. Since the binding energy of an assembly (with a polytropic equation of state) initially in a nonequilibrium state is less than that of a polytrope of the same mass, its material will not settle into as compact a configuration as the polytrope and the gravitational pull due to general relativity will not be as pronounced. Such a range was found to exist for the simple cases studied. It is not very wide, but may be of importance in stellar evolution.

A rough criterion for predicting from the initial conditions whether or not such an assembly will collapse can be obtained by estimating whether an outer radius can be found for which the force due to the pressure gradient just balances the gravitational attraction. If we indicate quantities at the outer boundary at this turnaround time by an asterisk, we are asking whether the equation of hydrostatic equilibrium

$$\left(\frac{1}{\rho w}\frac{dP}{dR}\right)^*\left(1-\frac{2MG}{R^*c^2}\right)=-\frac{MG}{R^{*2}}-\frac{4\pi G}{c^2}P^*R^* \tag{21}$$

can be satisfied for any R^*. Equation (21) follows immediately from (17) if time derivatives are set to zero and the independent space variable is changed from μ to R. Barring negative pressures, it has no solution if $\Gamma=0$, i.e., if $2MG/Rc^2=1$, anywhere.

Under our boundary condition, $P^*=0$. We estimate $(1/\rho w)^*(dP/dR)^*$ by assuming first, that the internal energy of the assembly increases approximately adiabatically according to a γ law (the shocks which do occur change the adiabat very little), and second, by writing the expression as a constant, n, times the ratio of the average specific internal energy at turnaround, $\epsilon_0(R_0/R^*)^{3(\gamma-1)}$, to R^*. n will depend on the form of $P(R)$ at turnaround time and on γ, and should be of order unity. We define α as the ratio of R^* to the Schwarzchild radius R_s. With these assumptions, (21) becomes an algebraic equation for α:

$$\frac{\alpha^{3\gamma-3}}{\alpha-1}=n\left[\frac{2\epsilon_0}{c^2}\left(\frac{R_0}{R_s}\right)^{3\gamma-3}\right]\equiv nK. \tag{22}$$

K is specified by the initial conditions. This method fails for $\gamma=\frac{4}{3}$, for which, in any case, no stable relativistic polytrope exists.

Equation (22) is clearly only indicative of the situation to which the fall will lead. In particular, n is not constant. Furthermore the radius at which the balance between pressure gradient and force of gravity is most precarious, in critical cases, is not that of the outer mass point, which has been kept large by the zero boundary pressure. It occurs in the outer half of the material. Nevertheless, the minimum value of nK for which (22) has a real solution should give the order of magnitude of the minimum radius inside of which most of the mass can come to hydrostatic equilibrium. Physically, if $\alpha\sim1$, the quantity Γ which multiplies the pressure gradient term in (17) will fall significantly below unity at the time at which the mass should turn around; the term u^2/c^2 in Γ [see Eq. (12)] will have been reduced by the cumulative effect of the outward pressure gradient below its free-fall value of $2MG/Rc^2$. Since $R_s\sim R$, the difference between Γ and 1 will not be negligible. As a result, the pressure gradient becomes ineffective, and the assembly continues to collapse. Since the pull of gravity increases as the pressure gradient decreases, the effect is expected to be catastrophic. On the other hand, if α is significantly greater than 1, these effects will be small and collapse will be avoided.

[6] J. R. Oppenheimer and G. M. Volkoff, Phys. Rev. 55, 374 (1939).

The behavior of assemblies of 2.1 $M_\odot$, 21 $M_\odot$, and 210 $M_\odot$ was calculated, using the equation of state $P=2\rho\epsilon/3$, corresponding to an adiabatic index $\gamma=\frac{5}{3}$. The assemblies were started from rest and from uniform rest mass and internal energy densities. The choice of uniform initial conditions was made, in part, because assemblies which start from complete Newtonian equilibrium were found to be more difficult to follow on the computer, the regions of extreme curvature occurring close to the center thereby necessitating fine zoning and long computing times; and, in part, because gravitationally unstable configurations of astrophysical interest, while not known, are now held likely to occur at the center of highly evolved stars,[7,8] where the assumptions of uniform density and temperature may be no worse than any other guess.

All the assemblies collapsed for $K\leq 1$ and bounced for $K\geq 2$, where bounce is defined as a state in which all the material is either at rest or moving outward (Fig. 1). For uniform initial conditions, if R_0 is the initial outer radius, the values of ϵ_0/c^2 and of $2MG/R_0c^2$ determine the path of a given mass fraction $\mu/\mu_{\max}$ in the plane of R/R_0 and $t(2MG/R_0^3)^{1/2}$.

Calculations were then made on the collapse of cold neutron spheres, varying both the mass and the equation of state. The neutrons were started from densities for which the Fermi energy is well in the nonrelativistic range, and were assumed to follow the equation of state of a nonrelativistic degenerate Fermi gas ($\gamma=\frac{5}{3}$) to begin with. The value of K for which collapse occurred was then bracketed for three equations of state:

$$P=\tfrac{2}{3}\rho\epsilon(\gamma=5/3) \text{ throughout the density range} \quad \text{(i)}$$

$$\begin{aligned} P&=\tfrac{2}{3}\rho\epsilon, & \rho&<\rho^* \\ &=(1/13)(\rho-\rho^*)\epsilon+\tfrac{2}{3}\rho^*\epsilon, & \rho&>\rho^* \end{aligned} \quad \text{(ii)}$$
$$\text{with } \rho^*=1.7\times10^{15}\text{ g/cm}^3.$$

(ii) represents a "soft" high density neutron equation of state, $\gamma=14/13$. It is approximately the one used by Misner and Zapolsky[9] to fit calculations of Ambartsumyan and Saakian on processes converting a high kinetic neutron into a baryon at rest. As would be

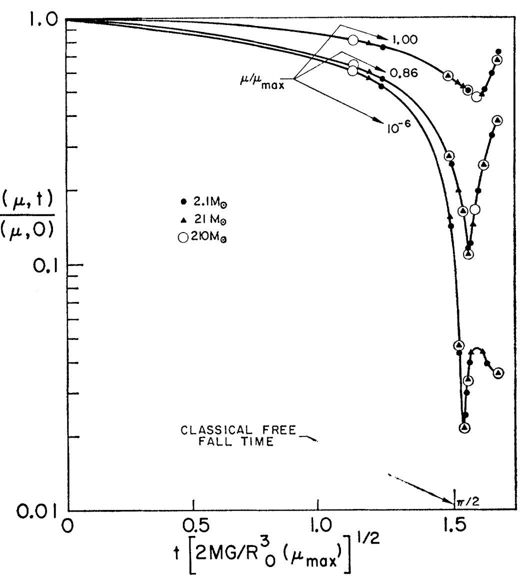

FIG. 1. $R(\mu,t)/R(\mu,0)$ versus $t[2MG/R^3(\mu\max,0)]^{1/2}$ for various mass fractions during the collapse and bounce of 2.1, 21, and 210 $M_\odot$, $\gamma=5/3$ spheres. The initial conditions in each case were $R_s/R=6.2\times10^{-3}$, $\epsilon_0/c^2=3.84\times10^{-5}$ corresponding to a K (Eq. 22) of 2.

expected for $\gamma<\frac{4}{3}$ (Ref. 6), an assembly in which ρ exceeds ρ^* does not come into equilibrium. The innermost region collapses to ever increasing densities.

$$\begin{aligned} P&=\tfrac{2}{3}\rho\epsilon \quad \rho<\rho^* \\ &=(\rho-\rho^*)\epsilon+\tfrac{2}{3}\rho^*\epsilon,\ \rho>\rho^*, \end{aligned} \quad \text{(iii)}$$
$$\text{with } \rho^*=5\times10^{14}\text{ g/cm}^3.$$

This choice represents a "hard core" high-density-neutron equation of state, $\gamma=2$. When $\gamma=2$, at very relativistic thermal energies, the speed of sound approaches the speed of light. However, at lower thermal energies, stiffer equations of state have been envisaged, notably one by Salpeter[10] discussed briefly in Sec. IV.

The results of these calculations are summarized in Table I. For equations of state (i) and (iii), $K\sim1$

TABLE I. Results of calculations on cold neutron spheres.

Equation of state	M ($M_\odot$)	$\mu_{\max}$ ($M_\odot$)	B ($M_\odot c^2$)	R_0 (km)	R_s/R_0	K	Collapse?	Final (g/cm³)	Maximum (g/cm³)
(i)	0.6890	0.6999	0.0109	32.0	0.0638	2.0	No	6×10^{14}	2×10^{15}
(i)	0.8924	0.9099	0.0175	34.88	0.0758	1.4	No	3×10^{15}	10^{16}
(i)	1.1024	1.1285	0.0261	37.426	0.0873	1.06	Yes	⋯	⋯
(i)	1.6321	1.6845	0.0524	42.656	0.1134	0.62	Yes	⋯	⋯
(ii)	0.8924	0.9099	0.0175	34.88	0.0758	1.4	Yes	⋯	⋯
(iii)	1.1024	1.1285	0.0261	37.426	0.0873	1.06	No	0.9×10^{15}	3×10^{15}
(iii)	1.3039	1.3388	0.0349	39.58	0.0976	0.84	Yes	⋯	⋯
				$\rho_0=10^{13}$ g/cm³					
				$\epsilon_0=3.64\times10^{18}$ erg/g					

[7] F. Hoyle and W. A. Fowler, Astrophys. J. **132**, 565 (1960).
[8] H. Y. Chiu, Phys. Rev. **123**, 1040 (1961).
[9] C. W. Misner and H. S. Zapolsky, Phys. Rev. Letters **12**, 635 (1964). Also, H. S. Zapolsky (private communication).
[10] E. E. Salpeter, Ann. Phys. (N. Y.) **11**, 393 (1960).

indicates the demarcation line between collapse and bounce. If masses of the same entropy and equation of state are compared, $\epsilon_0 R_0^{3(\gamma-1)}$ is constant, and K depends on the mass alone: for cold, nonrelativistic neutrons in particular:

$$K=\left(\frac{2\times10^{33}}{M}\right)^{4/3}, \quad =1 \text{ when } M\cong 1M_\odot.$$

Misner and Zapolsky[9], using $\gamma=5/3$, obtained a maximum stable polytropic mass of about 0.8 $M_\odot$.

Figures 2 through 7 show profiles of the 4-velocity, the circumference variable R, the rest mass density ρ, the quantities a and Γ, and the three terms in the equation of motion, Eq. (17), versus the radial variable μ at various times during the implosion and subsequent bounce of a 1.1 $M_\odot$ assembly with equation of

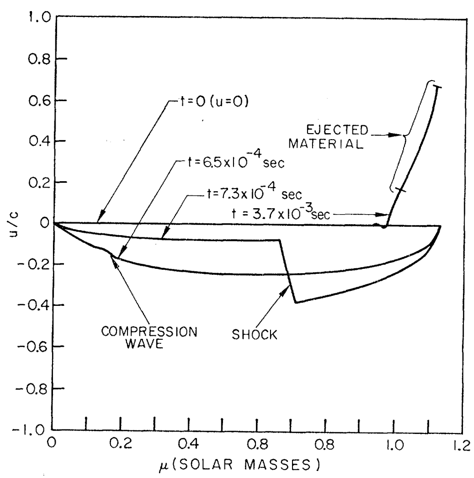

FIG. 2. u/c versus μ at several times during the collapse and bounce of a 1.1 $M_\odot$ sphere, equation of state (iii), with initially uniform density ($\rho_0=10^{+13}$) and specific internal energy ($\epsilon_0/c^2=4.04\times10^{-3}$) corresponding to $K=1.06$ [Eq. (22)].

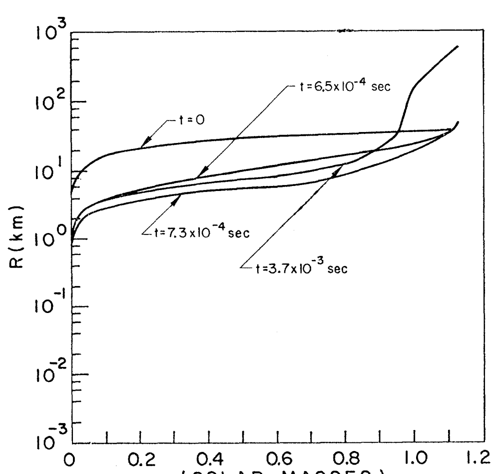

FIG. 3. R versus μ at several times during the collapse and bounce of the 1.1 $M_\odot$ sphere (see caption, Fig. 2, for initial conditions).

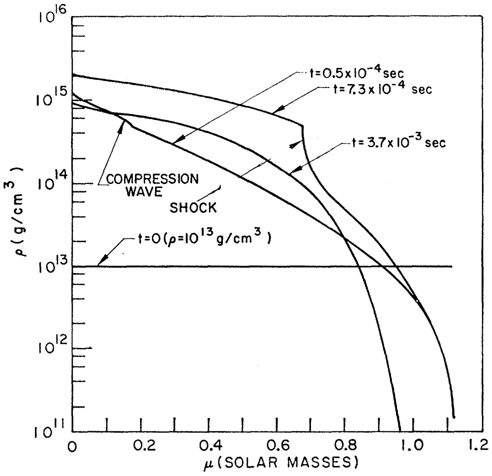

FIG. 4. ρ versus μ at several times during the collapse and bounce of the 1.1 $M_\odot$ sphere (see caption, Fig. 2, for initial conditions).

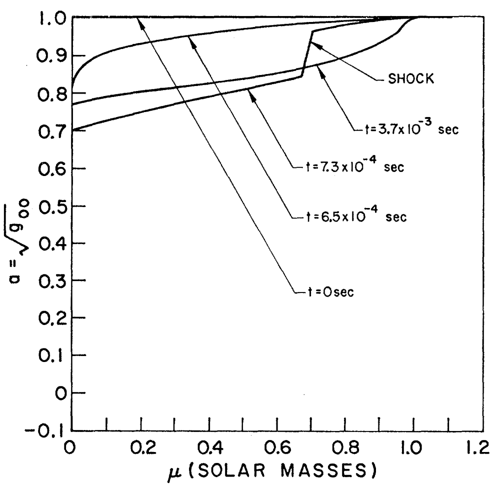

FIG. 5. $a=g_{00}^{1/2}$ at several times during the collapse and bounce of the 1.1 $M_\odot$ sphere (see caption, Fig. 2, for initial conditions).

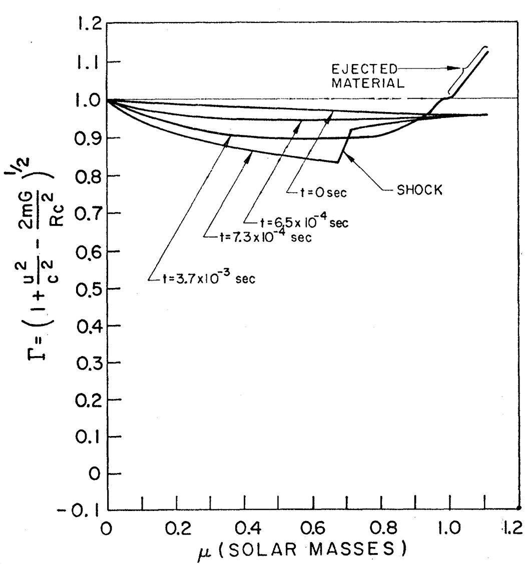

FIG. 6. Γ versus μ at several times during the collapse and bounce of the 1.1 $M_\odot$ sphere (see caption, Fig. 2, for initial conditions).

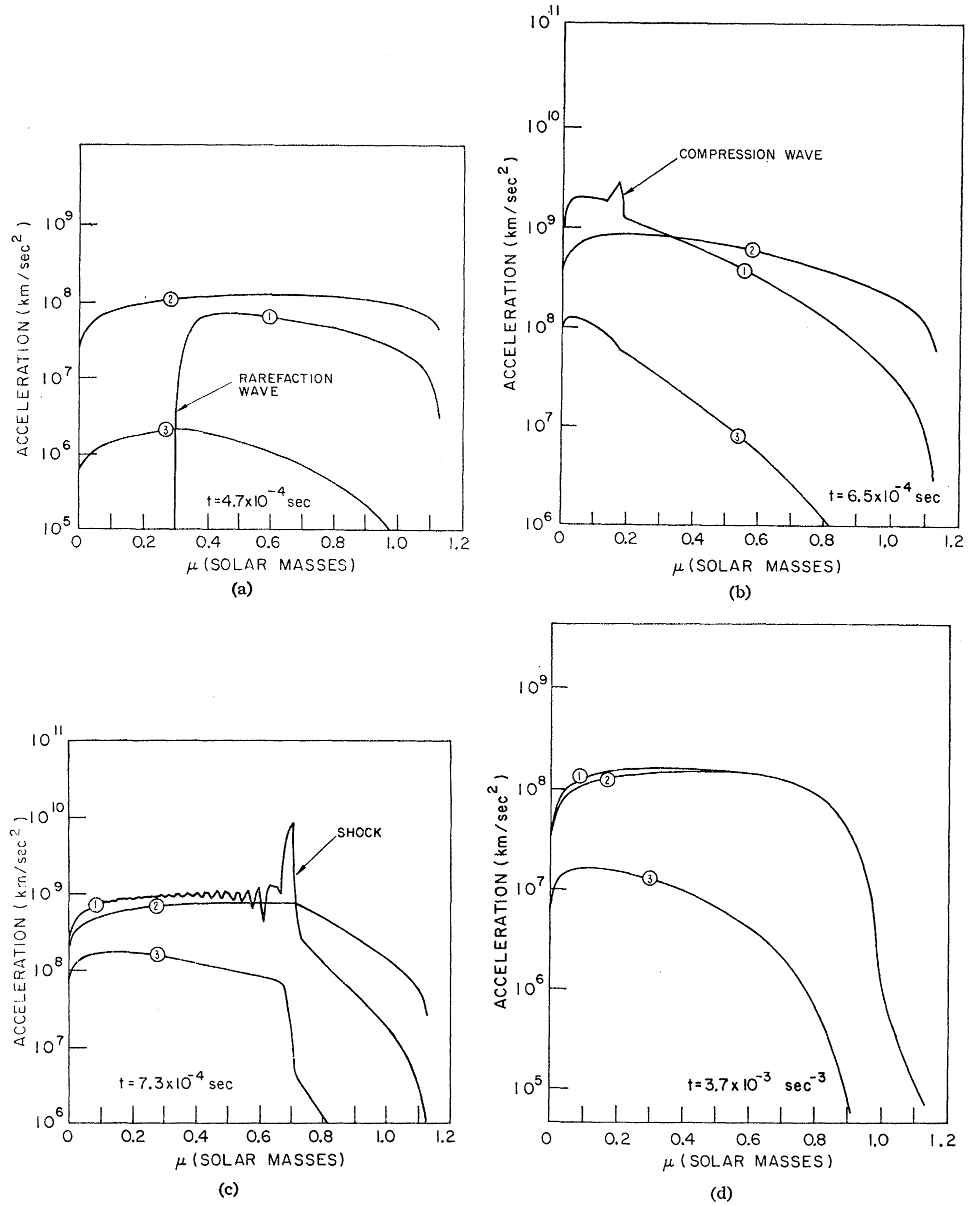

FIG. 7. The terms of Eq. (17) ($1=-4\pi aP'R^2\Gamma/w$, $2=amG/R^2$, $3=4\pi aPGR/c^2$) at various times during the collapse of the 1.1 $M_\odot$ sphere. (Initial conditions are given in the caption of Fig. 2). Figure 7(a) ($t=4.7\times10^{-4}$ sec) shows the initial rarefaction wave proceeding from the outside toward the center. In 7(b) ($t=6.5\times10^{-4}$ sec) the rarefaction has reached the center and a reflected compression wave can be seen. In 7(c) ($t=7.3\times10^{-4}$ sec) the rarefaction has steepened into a shock; the oscillations are numerical in origin. In 7(d) ($t=3.7\times10^{-3}$ sec) the shock has reached the outer surface and blown off $\sim$0.1 $M_\odot$. The acceleration terms are in equilibrium.

state (iii). Figures 8 through 13, which show the variations of similar quantities in a case of collapse, are discussed in part B of this section.

In several of the assemblies which bounced, some material was moving at more than escape velocity at the time of the last configuration calculated (Fig. 2). The upper limit to the amount of material which can escape from an assembly of initial binding energy B_0 and initial mass μ_0 is given from the conservation of energy and of rest mass by

$$B_P(\mu)=B_0(\mu_0)\,, \tag{23}$$

where $B_P(\mu)$ is the binding energy of a relativistic polytrope of rest mass μ, the highest binding energy possible for an assembly of that rest mass. For $\gamma=5/3$, this polytropic binding energy is about $0.04c^2M_\odot$ at the maximum stable polytropic mass of about $0.8M_\odot$, and goes to $\sim$0 at $0.3M_\odot$.[9]

While not enough relativistic polytropic configurations are available at this time to make a thorough survey, the problems run appear to allow escape of an amount of the order of the maximum mass allowed by Eq. (23). For instance, the $0.7M_\odot$ problem, which has an initial binding energy of $0.01c^2M_\odot$ allows escape of at least $0.052M_\odot$, together with about $0.003c^2M_\odot$ of excess kinetic energy over that needed for escape. The remaining $0.65M_\odot$ has a binding energy of

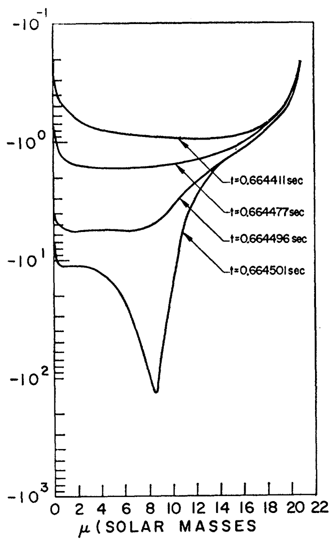

FIG. 8. u/c versus μ at various times during the collapse from rest of a $\gamma=5/3$, 21 $M_\odot$ sphere having an initially uniform density ($\rho_0=10^7$ g/cm^3) and specific internal energy ($\epsilon_0/c^2=9.61\times10^{-7}$). These initial conditions give $2MG/R_0c^2=0.0062$ and K [Eq. (22)]$=0.05$.

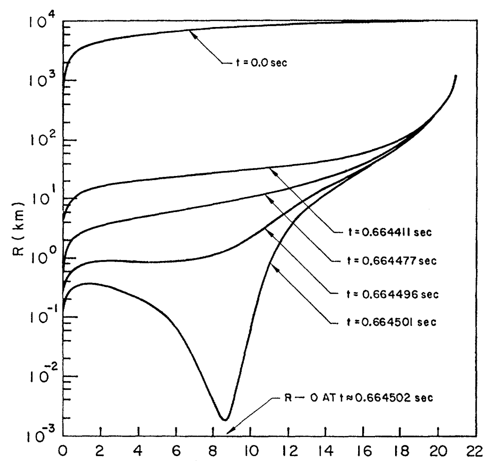

FIG. 9. R versus μ at times during the collapse of the 21 $M_\odot$ sphere (see caption, Fig. 8 for details of the initial configuration) The approach of R to zero at $\mu=8.5\ M_\odot$ and $t\approx0.6645$ sec is shown in Fig. 15.

$0.013c^2M_\odot$, as compared with $0.018c^2M_\odot$ for a polytrope of that mass.

B. Description of Continued Collapse

Continued collapse is characterized by material falling inside "its own" Schwarzchild radius,

$$R_s(\mu)=[2m(\mu)G]/c^2>R(\mu). \tag{24}$$

This event occurs first, in our coordinate time, at a point inside the assembly. The Schwarzchild radius there does not have the same clear meaning which it has when calculated for the mass of the whole assembly. The rate at which light signals are propagated inside the assembly is discussed in Sec. IV.

While the continuation of collapse of any part of the assembly past its Schwarzchild radius may take an infinite time as measured by clocks at infinity, it is of some theoretical interest to see how the hydrodynamic quantities and the geometry evolve during this collapse. As was suggested by Oppenheimer and Snyder,[11] this behavior is qualitatively similar to that which occurs when the pressure is zero.

The decrease in the pressure gradient term of Eq. (17) that occurs when Γ falls significantly below unity leads quite rapidly to a condition where the equations governing the motion of the material are

$$\dot{u}\cong-amG/R^2,\quad u^2\cong2mG/R, \tag{25}$$

replacing (17) and (12), respectively Eq. (25) has the

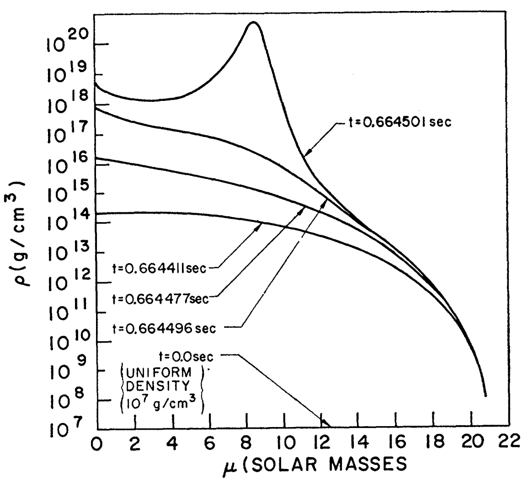

FIG. 10. ρ versus μ at times during the collapse of the 21 $M_\odot$ sphere (see caption, Fig. 8 for details of the initial configuration).

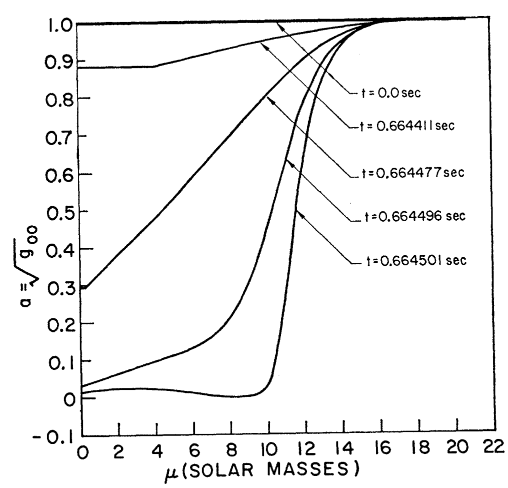

FIG. 11. $a=\sqrt{g_{00}}$ versus μ at times during the collapse of the 21 $M_\odot$ sphere (see caption, Fig. 8 for details of the initial configuration).

[11] J. R. Oppenheimer and H. Snyder, Phys. Rev. 56, 455 (1939).

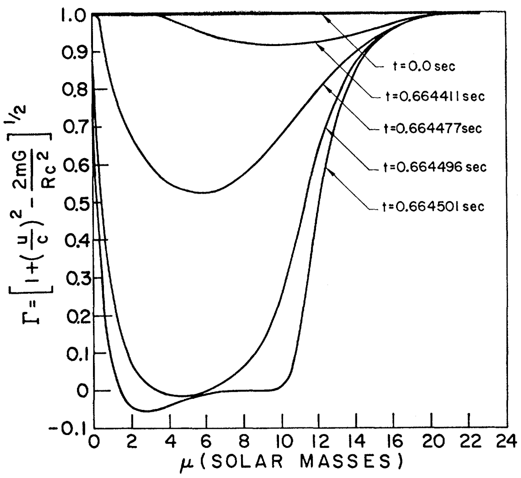

FIG. 12. Γ versus μ at times during the collapse of the 21 $M_\odot$ sphere (see caption, Fig. 8 for details of the initial configuration).

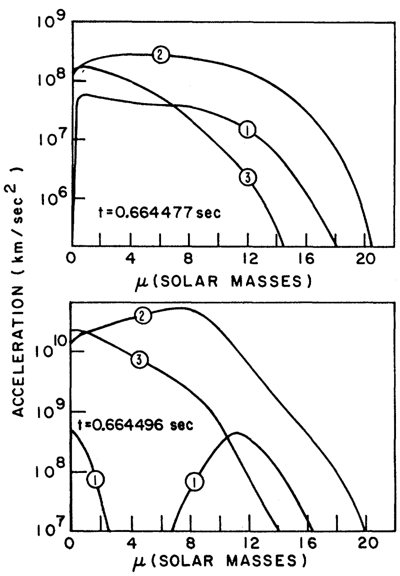

FIG. 13. The three terms in the equation of motion (17), $1=-4\pi aP'R^2\Gamma/w$, $2=aMG/R^2$, $3=4\pi aPGR/c^2$, versus μ at two times during the collapse of the 21 $M_\odot$ sphere (see caption, Fig. 8). The progressive failure of the pressure gradient term is clearly seen by comparing the upper and lower figures.

solution

$$u^2R=\frac{\dot{R}^2R}{a^2}=2mG,\quad \text{a constant in time.} \tag{26}$$

Each shell, $d\mu$, of material for which R_s has become much larger than R therefore falls freely since the pressure gradient term through which neighboring shells interact has become vanishingly small. The interaction by means of Eq. (15), for $T_1{}^k{}_{;k}$ is also small. In any case, since P' no longer affects the motion, (15) can only affect the way in which proper times compare in neighboring regions. In this connection, we recall that $\dot{R}$ is the time rate of change of the circumference variable. The sum of local measurements of radial distances,

$$r_p=\int_0^\mu \frac{d\mu}{4\pi\rho R^2}=\int_0^R \frac{dR}{\Gamma} \tag{27}$$

is becoming larger rather than smaller.

Differentiating (26) with respect to μ and using (18), we obtain

$$\dot{\rho}/\rho=-\tfrac{3}{2}(\dot{R}/R)-\tfrac{1}{2}(\dot{R}m'/R'm). \tag{28}$$

m'/m can be evaluated by using the $T_0{}^0$ and $T_1{}^1$ equations, (4) and (5), which give

$$\dot{R}m'/R'=-\dot{m}\rho(c^2+\epsilon)/P.$$

In our approximation, $\dot{m}/m\rightarrow 0$ while $\rho(1+\epsilon/c^2)/P$ remains finite. Hence, (28) gives

$$\rho R^{3/2}=\text{constant in time.} \tag{29}$$

So long as there is no interaction between neighboring materials, no shock forms, and the entropy at each mass point remains constant. Hence

$$\begin{aligned}\epsilon R^{3(\gamma-1)/2}&=\text{constant in time},\\ aR^{-3(\gamma-1)/2}&=\text{constant in time},\end{aligned} \tag{30}$$

where the second equation above also requires that the specific enthalpy w becomes very large compared with 1. Substituting for a from (30) into (26) and integrating gives:

$$\begin{aligned}R^{3-3/2\gamma}&=R_0{}^{2-3/2\gamma}[R_0-(3-\tfrac{3}{2}\gamma)|\dot{R}_0|],\quad &\gamma<2\\ R&=R_0\exp(-|\dot{R}_0|t/R_0), &\gamma=2\end{aligned} \tag{31}$$

where R_0, $\dot{R}_0$ are the values of R and $\dot{R}$ measured at the given mass point sometime after free fall begins, t being measured from that time.

For $\gamma<2$, the collapse therefore takes place in a finite interval of coordinate time, which is different for each shell of material. The fact that densities and pressures go to ∞ as R goes to 0 does not alter these conclusions, as the pressure gradient term, $P'R^2\Gamma/w$, goes to zero there as $RR'-\text{const } R'^2$.

All of these extrapolations are verified by the machine calculations. Figures 8 through 13 show, for the following case

$$M=21M_\odot,\quad R_0=10^4 km,\quad K=0.05,\quad p=\tfrac{2}{3}\rho\epsilon,$$

the same quantities as were shown in Figs. 2 through 7 for an assembly which bounced. We note that eventually Γ and R' become negative, and the surface area of concentric spheres decreases as one moves outward in μ space.

This curvature can also be obtained if it is assumed that ρ and ϵ are spatially uniform. The integration of the field equations then leads to an implicit equation for R as a function of μ:

$$\mu=2\pi\rho R_c[-R(R_c^2-R^2)^{1/2}+R_c^2\sin^{-1}(R/R_c)],$$

$$R_c=\left[\frac{3c^2}{8\pi G\rho(1+\epsilon/c^2)}\right]^{1/2}. \quad (32a)$$

For assemblies of rest mass exceeding some critical value

$$\mu_c=\pi^2\rho R_c^3, \quad (32b)$$

R decreases with increasing μ outside $\mu=\mu_c$ while, at $\mu=\mu_c$, $R=R_s$. The Schwarzchild radius of the assembly decreases with increasing μ even more rapidly than R, so that for $\mu>\mu_c$ we have $R>R_s$ and the addition of rest mass causes the Schwarzchild radius to retreat back inside the assembly. If negative pressures are allowed, this configuration can be static, and is then one of the Schwarzchild interior solutions.

Figure 14 shows the ratio of the Schwarzchild radius $R_s(\mu)$, defined by (24), to R, as a function of μ at various times during the collapse. We note, by comparing Figs. 12 and 14, that the region of negative Γ is inside the region where $2mG/Rc^2>1$. Figure 15 shows R and $\dot{R}$ versus coordinate time for the point at which R first approaches zero.

IV. DISCUSSION

The results described, although preliminary, lead to the conclusion that the upper mass limit for stability of a bound system against relativistic gravitational collapse is of the same order of magnitude whether calculated for falling material with a finite amount of kinetic energy or for a static configuration. While the excess kinetic energy of the falling material does offer the possibility of throwing off mass and leaving behind a core light enough to be stable, in order for this possibility to be realized, the pressure gradient must overcome the pull of gravity at the point of separation between what is to become the core and what is to be thrown off. If the pressure does not become high enough to do the job until the point of separation is at about the Schwarzchild radius for the mass enclosed, then the mechanism for turning material around fails. Static configurations near the limit of stability are only a few Schwarzchild radii in extent, so that our criterion for failure of the pressure gradient will lead to about the same maximum masses as the equilibrium calculations.

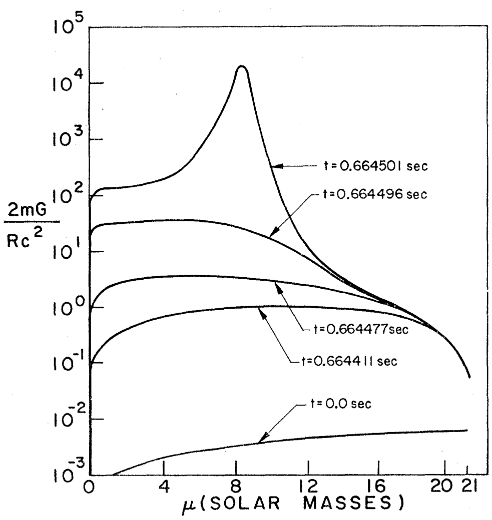

FIG. 14. $2MG/Rc^2=R_s(\mu)/R(\mu)$ versus μ at various times during the collapse of the 21 $M_\odot$ sphere (see caption, Fig. 8 for details of initial conditions).

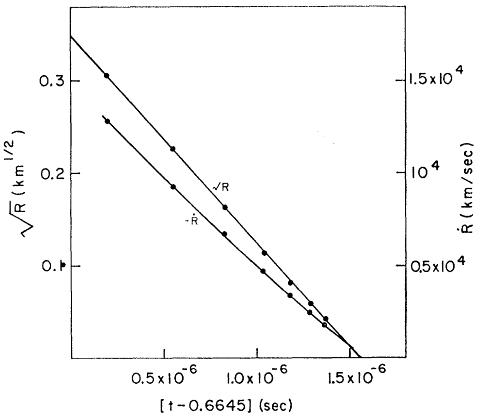

FIG. 15. $[R(\mu)]^{1/2}$ and $\dot{R}(\mu)$ versus t during free fall at $\mu=8.5$ $M_\odot$, the point where R first approaches zero for the 21 $M_\odot$ collapse. $R^{1/2}$ is linear in t as is predicted by Eq. (31) with $\gamma=5/3$.

For the case of complete collapse described above, $m(\mu)$ approaches a finite limit at the value of μ where first $R\to 0$. This limit is, however, greater than any value that m has had at that point earlier. This is required by Eq. (5), $\dot{R}$ being negative everywhere or, in the limit, 0. Therefore, in spite of the fact that there are negative contributions to the mass enclosed between the two values of μ for which $R=0$ (see Figs. 9 and 16), it does not seem possible, at least under the circumstances of our problem, for this mass to disappear and leave flat space behind.

The path of light signals through the collapsing assembly was calculated by integrating numerically:

$$(d\mu/dt)_{ds=0}=\pm 4\pi\rho R^2 ac \quad (33)$$

during the collapse, for signals started at regular intervals from the center and from the outside of the assembly. The results are shown in Fig. 17. Light signals do not leave the region where $2mG/Rc^2>1$, although they enter it in finite coordinate time. The region where $\Gamma<0$ is entirely enclosed by the region where $2mG/Rc^2>1$.

If $\Gamma<0$ in some element of rest mass, the total energy there

$$c^2dm=\Gamma(c^2+\epsilon)d\mu \quad (34)$$

is negative. The partial annihilation of $d\mu$, if permitted, would not change the sign of the total energy. Neither would an increase of ϵ. Since $\Gamma=0$ at the boundary of regions of negative Γ, pressure gradients could not push the material out of such regions. The annihilation of material at the center of the assembly, where $\Gamma>0$, and the subsequent transport of radiation, either into or possibly through the region of negative Γ, may provide a means for reducing m [see Eqs. (9), (11), (12)] but the effect of such reduction on the gravitational binding of a region of negative total energy is unclear.

Whether radiation can proceed from a region where $\Gamma<0$ to a region where $2mG/Rc^2<1$ and hence escape the assembly is also unclear. Configurations described by Eq. (32) (for $\mu>\mu_c$) do contain a region next to the outer boundary where both $\Gamma<0$ and $2mG/Rc^2<1$ obtain but such a region might not be physically realizable as it requires Γ to change sign at its boundary. We have not obtained such regions in our calculations. They would seem to be ruled out by Penrose's proof[12] that the null geodesics issuing from a trapped 2-surface converge toward the future, together with Hernandez and Misner's proof[13] that the Schwarzchild surface inside the matter is such a trapped surface.

The relevance of these calculations to astrophysical questions is now being studied. The effects of asphericity, of heat transfer by neutrinos or radiation, of pair creation and annihilation, and of interaction with outlying material must in general be treated. One of the simple results obtained so far may nevertheless be applicable. Supernovae are now presumed to be occasioned by the inward fall of a fraction of the highly

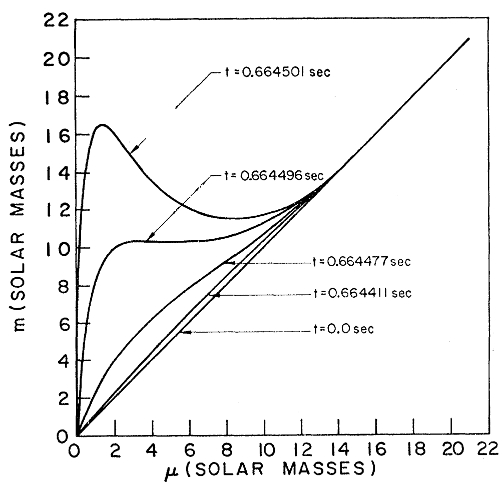

FIG. 16. $M(\mu)$ versus μ at various times during the collapse of the 21 $M_\odot$ sphere (see caption, Fig. 8 for details of the initial conditions).

[12] R. Penrose, Phys. Rev. Letters **14**, 57 (1965).

[13] Hernandez and C. W. Misner, Astrophys. J. (to be published).

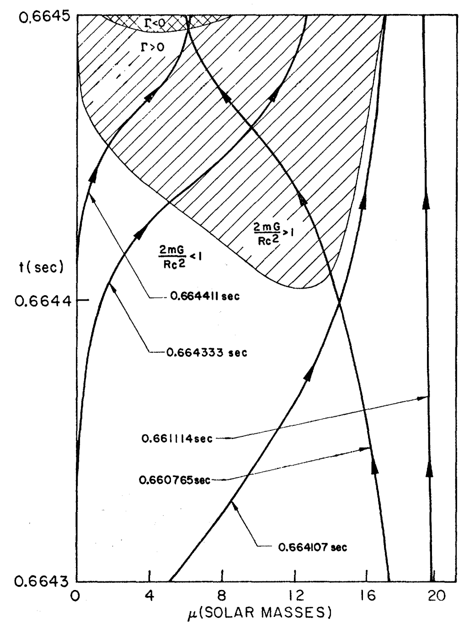

FIG. 17. Light cones (arrows) for the 21 $M_\odot$ collapse (see caption, Fig. 8 for details of initial configuration). Each signal is labeled with its time of origin.

evolved core of certain stars.[7,8] According to at least one model of this evolution, due to Colgate and White,[14] the amount of material which falls far enough so that its gravitational field must be corrected for general relativistic effects is of the order of magnitude of one to two solar masses. This occurs because it is mass of this order of magnitude which first fails to support itself in a Newtonian gravitational field upon cooling. We have followed the fall of a 1 $M_\odot$ core of this type, using the initial conditions obtained by Colgate and White from the classical evolution of a star of total mass $2M_\odot$, and also using a fit to Salpeter's equation of state.[10] The core still bounced. Whether enough of the energy released by neutrinos during the collapse and bounce would be absorbed in the (very high density) surrounding medium to prevent its falling on the core and thereby collapse it, remains to be calculated.

ACKNOWLEDGMENTS

We would like to thank S. A. Colgate, J. Fletcher, R. Lindquist, C. W. Misner, E. Teller, and, most particularly, J. A. Wheeler, for their encouragement and for very helpful discussions.

Earl Tech gave us considerable assistance with the computations.

[14] S. A. Colgate and R. H. White, University of California Lawrence Radiation Laboratory Report UCRL-7777 (1964) (to be published).